

# Vetoed jet clustering: The mass-jump algorithm

Martin Stoll

Department of Physics, University of Tokyo, Bunkyo-ku, Tokyo 113-0033, Japan

## Abstract

A new class of jet clustering algorithms is introduced. A criterion inspired by successful mass-drop taggers is applied which prevents the recombination of two hard prongs if they experience a substantial jump in jet mass. This veto effectively results in jets with variable radius in dense environments. Differences to existing methods are investigated and it is shown for boosted top quarks that the new algorithm has beneficial properties which can lead to improved tagging purity.

# 1 Introduction

The Large Hadron Collider (LHC) will restart in 2015 with unprecedented center-of-mass energy, pushing the window to find new particles beyond the Standard Model (SM) wide open. Practically all processes – SM or hypothetical – contain quarks or gluons in the final state and it is important that they can be reconstructed reliably. These coloured partons undergo parton showering and hadronization before they leave a signal in the detector. In order to make sense of experimental data it is therefore necessary to collect nearby radiation into jets, which are then assumed to correspond to their initiating (hard) partons.

Whenever jets are used as input for an analysis, the significance of the results crucially depends on the validity of this kinematic correspondence. Hence there has been ongoing effort to construct new and improved jet algorithms that are infrared and collinear safe, most of which proceed via sequential recombination [1, 2, 3, 4, 5, 6] or cones [7, 8, 9, 10], or follow completely different original ideas [11, 12, 13]. In the majority of these algorithms, jets are constructed with fixed angular size  $R$ , defined between two particles as  $\Delta R = \sqrt{\Delta\eta^2 + \Delta\phi^2}$  where  $\Delta\eta$  and  $\Delta\phi$  are the distances in pseudorapidity and azimuthal angle, respectively.

Despite this splendour of algorithms to select from, choosing the optimal jet radius is always a compromise [14] as it may be different for jets of different energy or position in the detector. Ref. [15] consequently proposes to employ a variable clustering radius instead, which in this case is taken inversely proportional to the jet transverse momentum,  $R \propto 1/p_\perp$ . An entirely different approach is taken by mass-drop tagging algorithms [16, 17, 18]. They address heavy resonances which are so highly boosted that their subsequent decay products cannot reasonably be resolved with conventional jet algorithms. Due to the high center-of-mass energy of the LHC, boosted top quarks, Higgs bosons, etc. are expected to be copiously produced during the upcoming run. To tag these resonances, it is possible to capture all decay products in a large-radius fat jet and apply substructure methods. The basic idea states that a jet should be broken up into two separate subjects if the jet mass experiences a significant drop in the procedure. These algorithms allow to identify hard substructure without referring to a fixed (sub)jet radius and turned out to perform very well in Higgs boson and top quark tagging (see e.g. [19, 20, 21] for reviews). Implicitly, a  $p_\perp$ -dependent subjet radius is given by the mass cut, as the characteristic separation between the daughters of an energetic resonance is  $\Delta R_{\text{daughters}} \gtrsim 2m_{\text{mother}}/p_\perp$ .

In this paper, we supplement existing jet algorithms with a recombination veto which may prevent further clustering at a jet radius smaller than the given  $R$ . The working principle is similar to mass-drop tagging: if the recombination of two jet candidates leads to a significant mass jump, they should be resolved separately. In contrast to algorithms with variable radius, the veto is a property of two jets, i.e. the effective clustering radius now also depends on the jet's vicinity. This way well-separated jets are clustered conventionally with only small deviations, whereas on the other hand the merging of two hard prongs into a heavy resonance is vetoed.

This paper is organized as follows. In Section 2, the mass-jump algorithm is motivated and

described in detail. Throughout the paper, we focus on consequences of the recombination veto in comparison to both classic jet algorithms as well as mass-drop taggers. In Section 3, we first evaluate the performance for well-separated jets, and then turn to the highly boosted regime. Beneficial properties for top quark tagging are pointed out. Conclusions are drawn in Section 4.

## 2 The algorithm

### 2.1 Review: Mass-drop unclustering

Developed to identify boosted Higgs bosons decaying into a pair of bottom quarks, the BDRS Higgs Tagger [16] established the family of mass-drop tagging (MDT) algorithms. It targets the 2-prong substructure of a large jet to identify the decay of a heavy resonance. Its modified 3-prong variant, the HEPTopTagger [17], enforces the following iterative procedure to act on a given fat jet clustered with the Cambridge/Aachen jet algorithm [4, 5].

- Un-do the last clustering of the jet  $j$  into  $j_1, j_2$  with  $m_{j_1} > m_{j_2}$ .
- If a significant mass drop occurred,  $m_{j_1} < \theta \cdot m_j$ , both  $j_1$  and  $j_2$  are kept as candidate subjects. Otherwise discard  $j_2$ .<sup>1</sup>
- Repeat these steps for the kept subjects unless  $m_{j_i} < \mu$ , in which case  $j_i$  is added to the set of output subjects.

The mass-drop (MD) procedure thus serves two purposes: It grooms the jet from (large-angle) soft radiation and applies a criterion to identify separate prongs based on jet mass. In the HEPTopTagger, the set of output subjects is then further processed and cuts applied. The default values of the two free parameters are chosen as  $\theta = 0.8$  and  $\mu = 30 \text{ GeV}$  [17, 23].

Note that the unclustering algorithm is designed to follow the cascade decay chain of the top quark,

$$t \rightarrow bW^+ \rightarrow bj j'. \quad (1)$$

At parton level the successive mass drops  $\tau = \frac{m_{j_1}}{m_j}$  are given by

$$\tau_1 = \frac{m_W}{m_t} \approx 0.46, \quad \tau_2 = \frac{m_q}{m_W} \approx 0, \quad (2)$$

hence the parameter  $\theta$  has to be chosen sufficiently large to incorporate the first decay. In case the unclustering proceeds via  $t \rightarrow j'(bj) \rightarrow j'bj$  one obtains

$$\tau'_1 = \frac{\sqrt{m_t^2 - m_W^2}}{2m_t} \Delta R_{bj} \quad (3)$$

---

<sup>1</sup>It has been pointed out [22] that following the heavier prong leads to a (small) wrong-branch contribution. This can be avoided by discarding the subject candidate with smaller transverse mass  $m_\perp^2 \equiv m^2 + p_\perp^2$  instead. As this modification is irrelevant for the remainder of this paper, we do not distinguish between the MDT and this modified mass-drop tagger (mMDT).

which is typically smaller than  $\tau_1$ .  $\Delta R_{bj} = \sqrt{\Delta\phi^2 + \Delta\eta^2}$  is the  $R$ -distance between the subjects  $b$  and  $j$ .

## 2.2 The mass-jump clustering algorithm

Commonly used sequential jet clustering algorithms define an infrared and collinearly safe procedure to merge particles into jets step by step. Termination of this sequential recombination is given (in the inclusive algorithms) in terms of a minimum jet separation  $R$ . All input particles (calorimeter towers) are labelled as jet candidates and a distance measure between pairs of two is defined,

$$d_{j_1 j_2} = \frac{\Delta R_{j_1 j_2}^2}{R^2} \min [p_{j_1 \perp}^{2n}, p_{j_2 \perp}^{2n}] , \quad d_{j_1 B} = p_{j_1 \perp}^{2n} , \quad (4)$$

where  $n = 1$  corresponds to the  $k_T$  algorithm [1, 2, 3],  $n = 0$  to the Cambridge/Aachen algorithm [4, 5], and  $n = -2$  to the anti- $k_T$  algorithm [6]. Sequential recombination then proceeds as follows:

1. Find the smallest  $d_{j_a j_b}$  among the jet candidates. If it is given by a beam distance,  $d_{j_a B}$ , label  $j_a$  a jet and repeat step 1.
2. Otherwise combine  $j_a$  and  $j_b$  by summing their four-momenta,  $p_{j_a j_b} = p_{j_a} + p_{j_b}$  ( $E$ -scheme, see e.g. Ref. [8]). In the set of jet candidates, replace  $j_a$  and  $j_b$  by their combination and go back to step 1.

Clustering eventually ends when all particles are merged into jets. The measure  $d$  serves two purposes here: First, it determines the order of recombination given by the pair with the smallest distance  $d_{j_a j_b}$  at each step. Second, it acts as an upper bound on the jet radius, because a minimal beam distance  $d_{j_a B}$  implies  $\Delta R_{j_a j_n} > R \forall$  jet candidates  $j_n$ .

We present a modification to these jet clustering algorithms which we call mass-jump (MJ) clustering. In the spirit of a reverse mass-*drop* procedure as outlined in the previous paragraph, “sub”jets are directly constructed by applying a veto at each recombination step,<sup>2</sup> where the parameter  $\theta$  now acts as a mass-*jump* threshold. After all input particles / calorimeter towers are labelled as *active* jet candidates, the recombination algorithm is defined as follows:

1. Find the smallest  $d_{j_a j_b}$  among active jet candidates; if it is given by a beam distance,  $d_{j_a B}$ , label  $j_a$  *passive* and repeat step 1.
2. Combine  $j_a$  and  $j_b$  by summing their four-momenta,  $p_{j_a+j_b} = p_{j_a} + p_{j_b}$  ( $E$ -scheme). If the new jet is still light,  $m_{j_a+j_b} < \mu$ , replace  $j_a$  and  $j_b$  by their combination in the set of active jet candidates and go back to step 1.  
Otherwise check the mass-jump criterion: If  $\theta \cdot m_{j_a+j_b} > \max[m_{j_a}, m_{j_b}]$  label  $j_a$  and  $j_b$  *passive* and go back to step 1.

---

<sup>2</sup>Separate measures for ordering variable and test (veto) variable were first introduced in Ref. [4].

3. Mass jumps can also appear between an active and a passive jet candidate. To examine this
  - a. Find the passive jet candidate  $j_n$  which is closest to  $j_a$  in terms of the metric  $d$ .
  - b. Then check if these two jet candidates would have been recombined if  $j_n$  had not been rendered passive by a previous veto, i.e.  $d_{j_a j_n} < d_{j_a j_b}$ .
  - c. Finally check the mass-jump criterion,  $m_{j_a+j_n} \geq \mu$  and  $\theta \cdot m_{j_a+j_n} > \max[m_{j_a}, m_{j_n}]$ .
 If all these criteria for the veto are fulfilled, label  $j_a$  *passive*. Do the same for  $j_b$ . If either of  $j_a$  or  $j_b$  turned passive, go back to step 1.
4. No mass-jump has been found, so replace  $j_a$  and  $j_b$  by their combination in the set of active jet candidates. Go back to step 1.

Clustering terminates when there are no more active jet candidates left. Passive candidates are then labelled jets. Note that for  $\theta = 0$  or  $\mu = \infty$  this algorithm is identical to standard sequential clustering without veto, which in this case can be reduced to steps 1 and 4.

### 2.3 Properties

The mass-jump veto only has an impact on jet candidates which are separated by  $\Delta R < R$  and whose combined mass would be above the (arbitrary) scale  $\mu$ . It is designed to resolve close-by jets (which could come from a boosted resonance decay such as  $W^\pm, Z, H, \dots$ ) separately. As the vetoed jets are excluded from further clustering, their jet radius is smaller than the parameter  $R$ , which now gives an upper bound. A lower bound is effectively induced by a finite threshold scale  $\mu$ .

There are several similarities and differences compared to MD unclustering. Fig. 1 schematically depicts a standard clustering sequence (e.g. of a hadronically decaying boosted top quark) and how the two algorithms act on the given event. The clustering sequence is to be read from right to left; hard prongs are depicted as straight lines, whereas wiggly lines symbolize soft radiation. The MDT sequentially unclusters a fat jet (which can be an actual large-radius jet or the whole event) from left to right, whereas the MJ algorithm starts from the fat jet's constituents and proceeds to the left. The final (sub)jets are indicated with red cones.

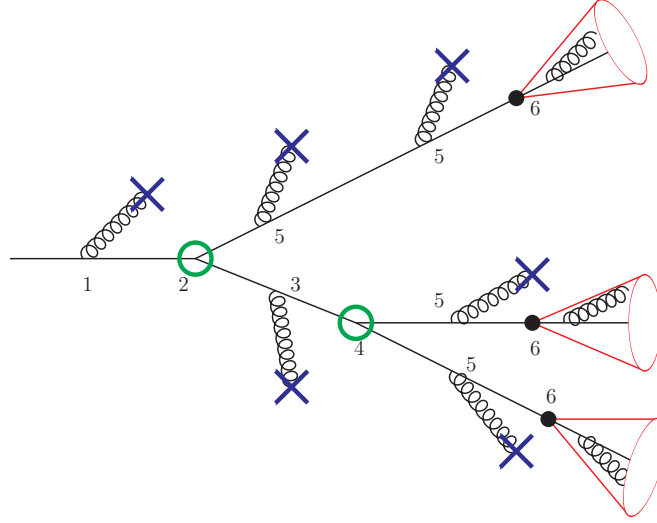
In the MDT algorithm (upper panel), starting from a fat jet soft radiation is groomed away (1) until at one unclustering step the mass-drop criterion is fulfilled, resulting in two subjets (2). The same grooming–tagging procedure continues for every prong which experiences a further mass-drop (3+4). More soft radiation is removed (5) until the subjet masses are below the threshold  $\mu$  (6). The remaining prongs are now labelled “subjets”.

MJ clustering (lower panel), on the other hand, is identical to standard clustering algorithms until the jet mass exceeds  $\mu$  (a).<sup>3</sup> Clustering continues (b) until the next recombination step would result in a substantial mass jump (c), at which step clustering is vetoed and the two

---

<sup>3</sup>Or the jet has reached its size given by the radius  $R$  – for the sake of comparison with the MDT procedure, we take  $R = \infty$  for the moment.

mass-drop unclustering of a fat jet



mass-jump clustering

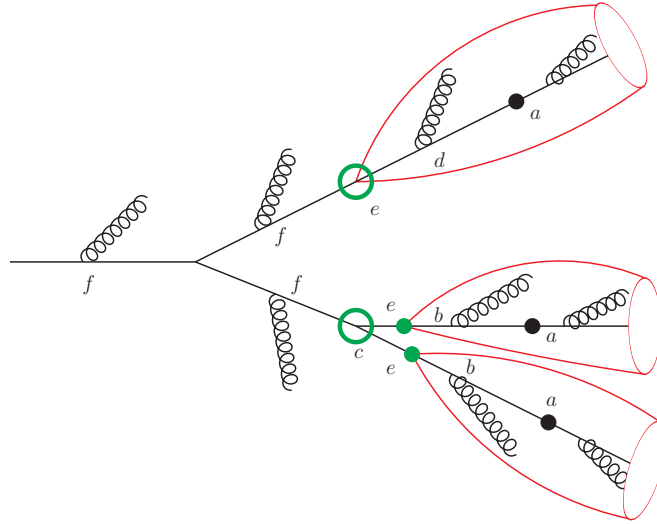


Figure 1: Key differences between MD unclustering (top) and MJ clustering (bottom) are visualized for a schematic clustering sequence (e.g. of a hadronically decaying boosted top quark). Sequential recombination is performed starting from the constituents at the right-hand side, such that in the upper panel the very left line symbolizes the whole fat jet which is then sequentially unclustered again (bottom panel: MJ clustering works its way from the constituent particles to the left). Inside the cluster sequence, hard prongs are depicted as straight lines, whereas wiggly lines symbolize soft radiation. Black dots denote the jet mass threshold  $m = \mu$ , and green circles indicate a mass drop (or mass jump). The final (sub)jets are indicated with red cones. The individual steps of the respective two algorithms (steps 1–6 for MD unclustering, steps a–f for MJ clustering) are described in the text.

prongs become passive. Active jet candidates continue clustering (d) unless a veto is called, which can also act against a (hypothetical) recombination with a passive jet (e). Jet clustering continues for the remaining particles, giving additional jets (f).

In the idealized case, the output jets of both algorithms are comparable but differ in two aspects. First, MDT subjets are groomed even after a mass drop until they reach  $m < \mu$  whereas MJ jets continue collecting radiation in the regime between  $m > \mu$  and the mass jump. Although this effect is expected to be absent for reasonable large values of  $\mu$ , if undesired it is straightforward to apply MDT-like grooming on the MJ jets. Second, the MJ clustering algorithm also returns jets which did not experience mass jumps (f) that are absent among MDT subjets (1,3,5). These can be desirable (well-separated jets for finite  $R$ ) or can be considered junk; in the latter case it is again straightforward to remove them as these are the only jets turned *passive* by the upper bound on the jet radius instead of a mass jump.

Also note the important property that MD unclustering experiences cascade mass-drops (cf. Sec. 2.1) while MJ clustering does not. This results in all mass jumps being among single hard prongs with a typical scale  $m_{\text{heavy resonance}}/\mu$ , i.e. the threshold parameter  $\theta$  can be chosen substantially lower.

### 3 Performance

#### 3.1 Sparse environment: QCD dijets

We compare the MJ clustering algorithm to its standard counterparts. In events with low multiplicity, the effect of the veto should be only limited. 100 QCD dijet events are simulated with Pythia8 [24] where the minimum parton transverse momentum at matrix element level is chosen  $\hat{p}_{\perp}^{\text{min}} = 150 \text{ GeV}$ . The analysis is implemented as a Rivet [25] plugin.

For jet clustering parameters  $R = 0.8$  and  $p_{\perp} \geq 50 \text{ GeV}$ , the three standard algorithms (anti- $k_T$ , Cambridge/Aachen and  $k_T$  algorithms as provided by FastJet [26]) agree very well in the number of jets  $n_{\text{std}}$ , which is 2 (in roughly one in two events) or above. We perform a parameter scan for the MJ clustering arguments  $\theta$  and  $\mu$ . Fig. 2 (bottom panel) shows the difference in the average number of jets per event ( $\Delta\bar{n} = \bar{n}_{\text{MJ}} - \bar{n}_{\text{std}}$ ). The mutual leading jets (i.e. the  $\min[n_{\text{MJ}}, n_{\text{std}}]$  jets with largest  $p_{\perp}$ ) in each event are matched, and differences between the MJ and standard algorithms are investigated on a jet-by-jet basis. For each pair  $(j_{\text{MJ}}, j_{\text{std}})$ , we obtain the  $R$ -distance ( $\Delta R_{j_{\text{MJ}}, j_{\text{std}}}$ ) and relative difference in transverse momentum ( $\Delta p_{\perp} = \frac{p_{\perp}^{\text{std}} - p_{\perp}^{\text{MJ}}}{p_{\perp}^{\text{std}} + p_{\perp}^{\text{MJ}}}$ ). The upper two panels of Fig. 2 show results of these two observables averaged over all matched jet pairs.

Differences between individual jets (upper two rows) are negligibly small in the small- $\theta$  and large- $\mu$  parameter regions for all three jet algorithms. This behaviour is expected as these are the limits where the veto is rendered ineffective. The closer the parameters are chosen to the strong-veto region ( $\theta \rightarrow 1$ ,  $\mu \rightarrow 0$ ), deviations between the vetoed and standard algorithms grow

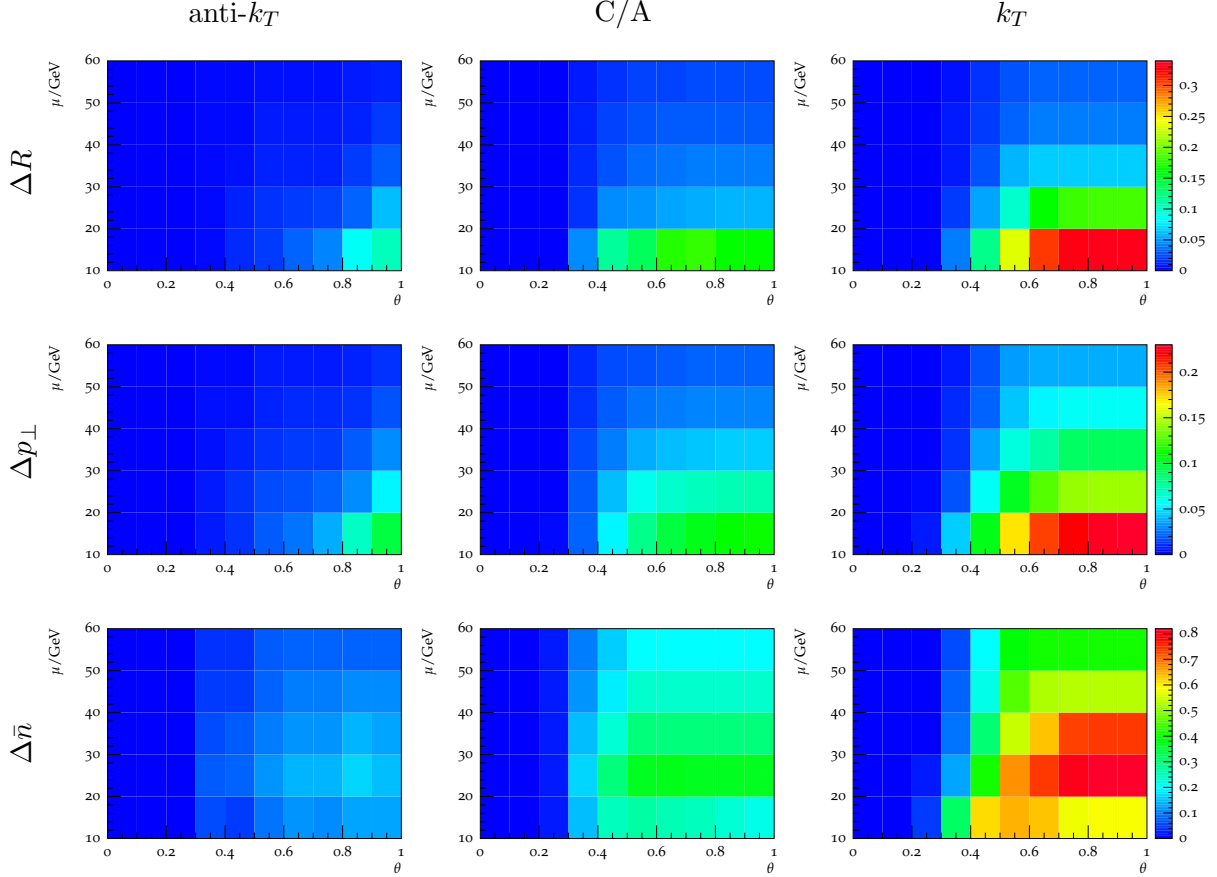


Figure 2: Comparison between MJ clustering and its standard counterparts for the anti- $k_T$  (left), C/A (middle) and  $k_T$  (right) algorithms. All jets were clustered with  $R = 0.8$  and  $p_\perp \geq 50$  GeV. The averaged observables  $\Delta R$ ,  $\Delta p_\perp$  and  $\Delta \bar{n}$  are shown from top to bottom for a range of parameters  $\theta$  and  $\mu$ .

larger. In particular for the  $k_T$  algorithm these differences can be substantial, namely  $\Delta R \sim 0.35$  and  $\Delta p_\perp \sim 0.25$  for the considered setup. The C/A and especially the anti- $k_T$  algorithm behave much more moderately under the MJ veto. For the latter, deviations only reach  $\Delta R \sim 0.1$  and  $\Delta p_\perp \sim 0.1$  even in the strong-veto region, and are almost absent in the bulk of parameter space.

Generally the differences between MJ vetoed and standard clustering are smallest for the anti- $k_T$  algorithm and largest for the  $k_T$  algorithm, with the C/A algorithm taking an intermediate position. This characteristic is directly related to the ordering of the cluster sequence, which is crucial in the MJ algorithm. If soft particles are clustered first ( $k_T$ ), it is very likely to induce fake substructure which will fulfill the mass-jump condition at the stage when these soft clusters are recombined. The anti- $k_T$  algorithm on the other hand clusters around hard prongs and therefore is much more robust, while the purely angular-based C/A algorithm is moderately prone to vetoing fake soft clusters.

The number of jets is naturally equal or larger in the vetoed algorithms compared to the



standard algorithms with equal jet clustering radius (Fig. 2 lower panels). If however the veto acts too strong, hard jets are split and may not pass the  $p_{\perp} \geq p_{\perp}^{\min}$  cut any more, resulting in a decreasing number of jets again. For large minimum transverse momentum, say  $p_{\perp} > 100$  GeV for our sample,  $\Delta\bar{n}$  ultimately becomes negative.

Also for other jet clustering radii and  $p_{\perp}$  thresholds, results are qualitatively very similar to the ones described above, so we omit further plots.

### 3.2 Busy environment: boosted top quarks

Tagging boosted top quarks is an important target in many current experimental studies and also an ideal playground to investigate the performance of MJ clustering in busy environments. In order to probe the moderately boosted energy regime and illustrate the algorithm, we simulate top pair production via a hypothetical heavy vector boson,

$$pp \rightarrow Z' \rightarrow t\bar{t} \rightarrow \text{hadrons} \quad (5)$$

for two different resonance masses  $m_{Z'} = 500$  and  $700$  GeV. These samples result in fat jet distributions (Cambridge/Aachen with  $R = 1.5$ ,  $p_{\perp} \geq 200$  GeV) steeply dropping in  $p_{\perp}$  ( $m_{Z'} = 500$  GeV sample) and peaking around moderate boosts of  $\sim 300$  GeV ( $m_{Z'} = 700$  GeV sample), respectively. Those fat jets are fed to the HEPTopTagger [17] which performs the following three-step procedure.

1. Subjets are obtained from the fat jet via mass-drop unclustering.
2. The subjets are filtered.
3. Cuts on subjet mass ratios determine whether or not the candidate is tagged as top.

For comparison with our veto algorithm, we apply the same algorithm but where the subjets are now obtained directly with MJ clustering starting from the fat jet's constituent particles. Steps 2 and 3 remain unchanged such that the difference in tagging performance can be directly compared. We take  $R = \infty$  and scan the parameter space in  $\theta$  and  $\mu$ . Results are based on each 10,000 signal and background events (QCD dijets with  $\hat{p}_{\perp}^{\min} = 150$  GeV) generated with Pythia8 and analyzed within Rivet. The resulting tagging efficiencies  $\epsilon = \frac{\#\text{tagged}}{\#\text{fat jets}}$  are shown in Fig. 3.<sup>4</sup>

Indeed the peak tagging efficiencies are equal for both algorithms. However, as argued in Sec. 2.3, MJ jet finding allows for well-performing top tagging in a much wider parameter range in  $\theta$ . The reason for this behaviour lies in the absence of an equivalent to the cascade mass drops experienced in MDT's (such as  $t \rightarrow bW^+ \rightarrow bj\bar{j}'$ ). This feature can also be directly seen in Fig. 3 where in the MDT case (left) the onset of top tagging is around  $\theta = 0.5 \approx \frac{m_W}{m_t}$ , whereas for MJ clustering (right) the characteristic scale is much lower. In particular, lower values of  $\theta$

---

<sup>4</sup>Fat jets which deviate too much from their Monte Carlo truth top quark ( $\Delta R_{j^{\text{fat}}, t^{\text{MC}}} > 0.6$ ) are ignored in signal events.

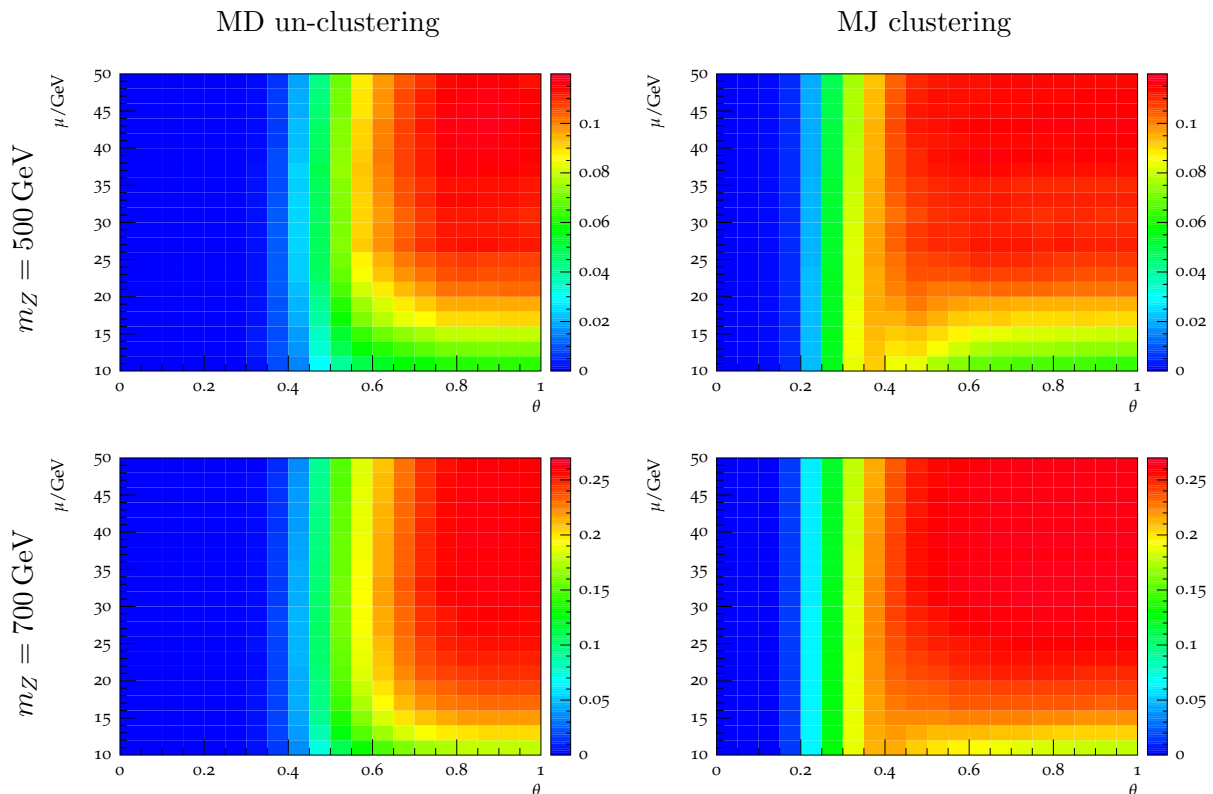


Figure 3: Top tagging efficiency  $\epsilon$  for the HEPTopTagger with MD un-clustering (left) and MJ clustering (right). For both algorithms the parameter space  $\theta, \mu$  is scanned. The top panels show signal rates for the  $m_{Z'} = 500$  GeV sample, the lower panels for the 700 GeV sample.

correspond to a much stricter identification of separate jets which might turn out beneficial for background rejection.

Fig. 4 compares the receiver-operating characteristic (ROC) curves of MJ clustering and MD unclustering in conjunction with the HEPTopTagger.<sup>5</sup> It is observed that signal tagging efficiency and background rejection coincide in the saturated parameter region at  $\epsilon_{\text{sig}} \approx 0.26$  and  $R = 1 - \epsilon_{\text{bkg}} \approx 0.991$  for the  $m_{Z'} = 700$  GeV sample, and at  $(0.12, 0.991)$  for the  $m_{Z'} = 500$  GeV sample, respectively. However due to the enlarged parameter space, the MJ algorithm outperforms the standard procedure and should be preferred in the transition (high-purity) region. This result is even more pronounced if limited detector resolution is taken into account. For our simple analysis, this is implemented by applying a cellular grid in  $\eta$ - $\phi$  space and re-placing all stable hadrons to the center of their respective cells. Apparently MJ clustering is flexible enough to avoid a decrease in performance under these circumstances as well.

<sup>5</sup>These curves are obtained from the full parameter scan. Among all setups  $(\theta, \mu)$  which give a similar signal tagging efficiency, only the one that yields the highest background rejection is picked and plotted.

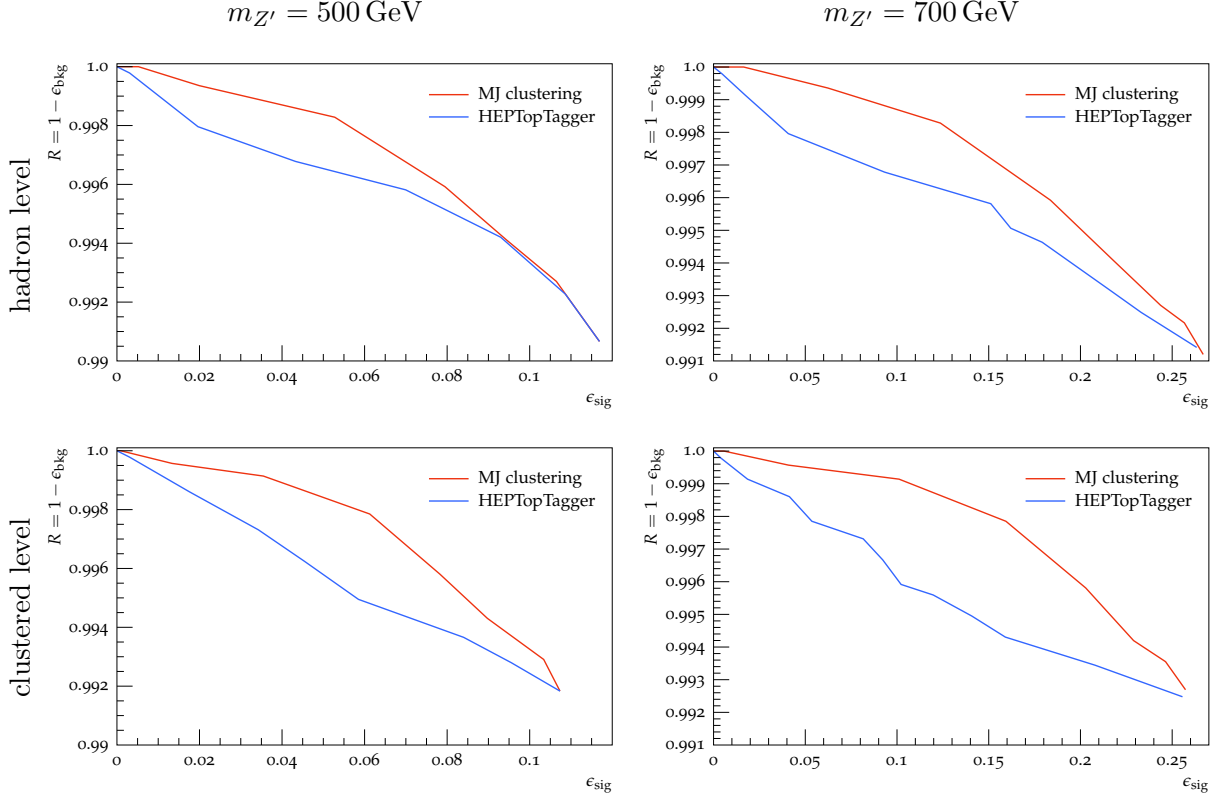


Figure 4: Receiver-operating characteristic (ROC) curves for top tagging using the HEPTopTagger. The MJ clustering algorithm (red) is compared to standard MD un-clustering (blue). From left to right, the upper panels show results at hadron level for the  $m_{Z'} = 500$  GeV and the 700 GeV sample, respectively. The lower panels are similar but obtained from hadrons centered into  $(0.1, 0.1)$  cells in  $\eta$ - $\phi$  space to emulate finite detector resolution. If high purity is desired, MJ clustering gives improved performance.

## 4 Conclusions

We developed and investigated a new jet clustering algorithm which includes a recombination veto based on jet mass. In this mass-jump (MJ) procedure, the clustering radius  $R$  now acts as an upper limit on jet size and the merging of two hard prongs is prevented. We showed that in sparse events with well-separated jets, the effect of the veto is very limited in a large range of parameter space. Also the anti- $k_T$  clustering algorithm is more robust against fake two-prong substructure than the Cambridge/Aachen and  $k_T$  algorithms. In the dense environment of hadronically decaying boosted top quarks, MJ clustering is comparable to mass-drop taggers (MDT) by which the veto was inspired in the first place; the main difference being that cascade mass drops as present in MDT's are avoided which allows for stricter threshold parameters. The larger parameter space then leads to improved ROC curves for the new MJ clustering in the context of the HEPTopTagger algorithm.

Vetoed clustering algorithms are a promising tool for collider experiments as they make room for more flexibility. The optimal jet clustering radius depends on various parameters such as the type of initiating particle, its energy or transverse momentum, and the surrounding topology of the event. The MJ veto automatically adjusts the jet radius such that hard substructure is separated into isolated jets. This feature may prove helpful in a variety of events where jets are not well-separated.

## Acknowledgment

The author is grateful to Koichi Hamaguchi for helpful discussion and also Go Mishima for comments on the manuscript. This work was supported by the Program for Leading Graduate Schools.

## References

- [1] S. Catani, Y. L. Dokshitzer, M. Olsson, G. Turnock and B. R. Webber, Phys. Lett. B **269**, 432 (1991).
- [2] S. Catani, Y. L. Dokshitzer, M. H. Seymour and B. R. Webber, Nucl. Phys. B **406**, 187 (1993).
- [3] S. D. Ellis and D. E. Soper, Phys. Rev. D **48**, 3160 (1993) [hep-ph/9305266].
- [4] Y. L. Dokshitzer, G. D. Leder, S. Moretti and B. R. Webber, JHEP **9708**, 001 (1997) [hep-ph/9707323].
- [5] M. Wobisch and T. Wengler, In \*Hamburg 1998/1999, Monte Carlo generators for HERA physics\* 270-279 [hep-ph/9907280].
- [6] M. Cacciari, G. P. Salam and G. Soyez, JHEP **0804**, 063 (2008) [arXiv:0802.1189 [hep-ph]].
- [7] G. F. Sterman and S. Weinberg, Phys. Rev. Lett. **39**, 1436 (1977).
- [8] G. C. Blazey, J. R. Dittmann, S. D. Ellis, V. D. Elvira, K. Frame, S. Grinstein, R. Hirosky and R. Piegaia *et al.*, hep-ex/0005012.
- [9] M. G. Albrow *et al.* [TeV4LHC QCD Working Group Collaboration], hep-ph/0610012.
- [10] G. P. Salam and G. Soyez, JHEP **0705**, 086 (2007) [arXiv:0704.0292 [hep-ph]].
- [11] D. Bertolini, T. Chan and J. Thaler, JHEP **1404**, 013 (2014) [arXiv:1310.7584 [hep-ph]].
- [12] H. Georgi, arXiv:1408.1161 [hep-ph].
- [13] S. F. Ge, arXiv:1408.3823 [hep-ph].
- [14] G. Soyez, JHEP **1007**, 075 (2010) [arXiv:1006.3634 [hep-ph]].
- [15] D. Krohn, J. Thaler and L. T. Wang, JHEP **0906**, 059 (2009) [arXiv:0903.0392 [hep-ph]].

- [16] J. M. Butterworth, A. R. Davison, M. Rubin and G. P. Salam, Phys. Rev. Lett. **100**, 242001 (2008) [arXiv:0802.2470 [hep-ph]].
- [17] T. Plehn, M. Spannowsky, M. Takeuchi and D. Zerwas, JHEP **1010**, 078 (2010) [arXiv:1006.2833 [hep-ph]].
- [18] S. Schaetzel and M. Spannowsky, Phys. Rev. D **89**, 014007 (2014) [arXiv:1308.0540 [hep-ph]].
- [19] A. Abdesselam, E. B. Kuutmann, U. Bitenc, G. Brooijmans, J. Butterworth, P. Bruckman de Renstrom, D. Buarque Franzosi and R. Buckingham *et al.*, Eur. Phys. J. C **71**, 1661 (2011) [arXiv:1012.5412 [hep-ph]].
- [20] A. Altheimer, S. Arora, L. Asquith, G. Brooijmans, J. Butterworth, M. Campanelli, B. Chapleau and A. E. Cholakian *et al.*, J. Phys. G **39**, 063001 (2012) [arXiv:1201.0008 [hep-ph]].
- [21] T. Plehn and M. Spannowsky, J. Phys. G **39**, 083001 (2012) [arXiv:1112.4441 [hep-ph]].
- [22] M. Dasgupta, A. Fregoso, S. Marzani and G. P. Salam, JHEP **1309**, 029 (2013) [arXiv:1307.0007 [hep-ph]].
- [23] C. Anders, C. Bernaciak, G. Kasieczka, T. Plehn and T. Schell, Phys. Rev. D **89**, 074047 (2014) [arXiv:1312.1504 [hep-ph]].
- [24] T. Sjostrand, S. Mrenna and P. Z. Skands, Comput. Phys. Commun. **178**, 852 (2008) [arXiv:0710.3820 [hep-ph]].
- [25] A. Buckley, J. Butterworth, L. Lonnblad, D. Grellscheid, H. Hoeth, J. Monk, H. Schulz and F. Siegert, Comput. Phys. Commun. **184**, 2803 (2013) [arXiv:1003.0694 [hep-ph]].
- [26] M. Cacciari, G. P. Salam and G. Soyez, Eur. Phys. J. C **72**, 1896 (2012) [arXiv:1111.6097 [hep-ph]].